Coexistence of bound and virtual-bound states in shallow-core to valence x-ray spectroscopies

Subhra Sen Gupta,[1,*] J. A. Bradley,[2] M. W. Haverkort,[3] G. T. Seidler,[2] A. Tanaka,[4] and G. A. Sawatzky[1]

[1]*Department of Physics and Astronomy, University of British Columbia, Vancouver, BC V6T 1Z1, Canada*

[2]*Department of Physics, University of Washington, Seattle, Washington 98105, USA*

[3]*Max Planck Institute for Solid State Research, Heisenbergstraße 1, D-70569 Stuttgart, Germany*

[4]*Department of Quantum Matter, ADSM, Hiroshima University, Higashi-Hiroshima 739-8530, Japan*

(Received 9 May 2011; published 10 August 2011)

With the example of the *non-resonant inelastic x-ray scattering* (NIXS) at the O_{45} edges ($5d \rightarrow 5f$) of the actinides, we develop the theory for *shallow-core to valence excitations*, where the multiplet spread is larger than the core-hole attraction, such as if the core and valence orbitals have the *same principal quantum number*. This involves very strong final state configuration interaction (CI), which manifests itself as huge reductions in the Slater-Condon integrals, needed to explain the spectral shapes within a simple renormalized atomic multiplet theory. But more importantly, this results in a cross-over from bound (excitonic) to virtual-bound excited states with increasing energy, within the same core-valance multiplet structure, and in large differences between the dipole and high-order multipole transitions, as observed in NIXS. While the bound states (often higher multipole allowed) can still be modeled using local cluster-like models, the virtual-bound resonances (often dipole-allowed) cannot be interpreted within such local approaches. This is in stark contrast to the more familiar core-valence transitions *between different principal quantum number shells*, where *all* the final excited states almost invariably form bound core-hole excitons and can be modeled using local approaches. The possibility of observing *giant multipole resonances* for systems with high angular momentum ground states is also predicted. The theory is important to obtain ground state information from core-level x-ray spectroscopies of strongly correlated transition metal, rare-earth, and actinide systems.

DOI: 10.1103/PhysRevB.84.075134 PACS number(s): 78.70.Ck, 78.20.Bh, 78.47.da, 78.70.Dm

I. INTRODUCTION

The actinides and their compounds are attracting serious attention from the condensed matter community due to their exotic properties.[1] Examples of these are the extremely rich phase diagram of Plutonium[2] and the unsolved "hidden-order" phase[3] of URu_2Si_2 below 17.5 K. Their properties interpolate between more itinerant 3*d transition metal* (TM) systems and more localized 4*f rare-earth* (RE) complexes,[4] and exhibit strong interplay between spin, charge, orbital, and lattice degrees of freedom. Thus, versatile experimental techniques are needed to unravel the physics operative in these systems. Core-level spectroscopies, like *x-ray absorption spectroscopy* (XAS), have been extremely successful in providing information regarding the ground state of TM and RE systems, relying largely on theoretical interpretations based on local correlated models with full multiplet effects[5] and atomic selection rules.

The success of such local multiplet models relies strongly on two facts : (1) the electronic structure of these strongly correlated systems is largely governed by local correlation physics and point group symmetry, and (2) the final state core-hole strongly binds the extra d or f electron, so that *all* core-valence multiplet states form *excitonic bound states*. However, core-valence excitations within the *same principal quantum number (n)-shell*, like the $5d \rightarrow 5f$ transitions in the actinides (or for that matter the $4d \rightarrow 4f$ transitions in the RE, or the $3p \rightarrow 3d$ transitions in TM compounds), pose a problem because the core-valence multiplet spread is ~20–25 eV, often much larger than the average core-hole valence-electron attractive potential (Q) itself. This pushes the higher lying terms of these multiplets up into the conduction band, "autoionizing" the extra f electron. Such mixing with band-structure or autoionization continua gives rise to very broad, virtual-bound *Fano-resonances*,[6] that cannot be interpreted in terms of local models. We note that this effect is distinct from those involving the decay of the core-hole itself, which have been elegantly described[7,8] for these *giant dipole resonances* (GDR).[10]

The strong hybridization of the $5f$ electrons with conduction band states requires detailed information about interatomic interactions and band structure effects, ruling out the usefulness of atomistic models. There have been attempts to interpret these broad, so called *giant-resonances* in terms of broad spin-orbit split multiplets in the final state,[11] but this may not be the complete picture. This is because the core-5*d* spin-orbit splitting between the $5d_{3/2}$ and $5d_{5/2}$ states in Th or U is of the order 6–8 eV, whereas the GDR is spread over an energy range of 15–20 eV, and it is hard to imagine that core-hole lifetime effects alone can account for this enormous spread. In this article, we emphasize that the structure of core-level excitations within the same n-shell, is fundamentally different from that between different n-shells, with the example of the $5d \rightarrow 5f$ *non-resonant inelastic x-ray scattering* (NIXS) in the actinides. We also show that the high-multipole transitions in NIXS to strongly bound core-valence multiplet states, unlike the dipole restricted transitions in XAS and *electron energy loss spectroscopy* (EELS), can still be treated within local models, but with strongly renormalized parameters, due to very large *configuration interaction* (CI) in the final state.

NIXS involves first order scattering at photon energies much larger than any typical atomic excitation edge ($h\nu \sim 6 - 10$ keV), arising from the $(e^2/2mc^2)\vec{A} \cdot \vec{A}$ term in the light-matter coupling.[12] The corresponding double differential cross-section is given by[12]

$$\frac{d^2\sigma}{d\omega_f d\Omega} = \left(\frac{d\sigma}{d\Omega}\right)_{Th} \cdot S(\vec{q},\omega), \qquad (1)$$

where, $(\frac{d\sigma}{d\Omega})_{Th}$ is the Thompson scattering cross-section for a free electron, while the material dependence is completely contained in the wave-vector ($\vec{q}$) and frequency (ω) dependent *dynamical structure factor*, $S(\vec{q},\omega)$, given by

$$S(\vec{q},\omega) = \sum_f |\langle f|e^{i\vec{q}\cdot\vec{r}}|i\rangle|^2 \delta(E_f - E_i - \hbar\omega), \qquad (2)$$

where, $\vec{q} = \vec{k}_i - \vec{k}_f$ is the *photon momentum transfer*, and $\hbar\omega = \hbar\omega_i - \hbar\omega_f$ is the *energy loss*, both transferred to the electronic system. Here $|i\rangle$ and $|f\rangle$ are the many-body initial and final states of the system, with energies E_i and E_f, respectively. The transition operator can be multipole expanded[13,14] as:

$$e^{i\vec{q}\cdot\vec{r}} = \sum_{l=0}^{\infty} \sum_{m=-l}^{l} i^l (2l+1) j_l(qr) C_m^{(l)*}(\theta_{\vec{q}},\phi_{\vec{q}}) C_m^{(l)}(\theta_{\vec{r}},\phi_{\vec{r}}), \quad (3)$$

where, $q = |\vec{q}|$ and $r = |\vec{r}|$, and $j_l(qr)$ are spherical Bessel functions, while $C_m^{(l)}(\theta,\phi)$ are renormalized spherical harmonics, both of order l. Due to angular momentum and parity selection rules, only terms with $|l_f - l_i| \leqslant l \leqslant (l_f + l_i)$ and $(l + l_i + l_f)$ *even*, survive in the infinite sum. As is evident from Eq. (3), NIXS can access transitions involving high-order multipole channels (l), unlike the dipole restricted XAS, the weight of each multipole being decided by the reduced (radial) matrix element $\langle 5f||j_l(qr)||5d\rangle = \langle R_{5f}(r)|j_l(qr)|R_{5d}(r)\rangle$. In Eq. (3) the angular part of the operator relating to the electron coordinates is the spherical harmonic $C_m^{(l)}(\theta_{\vec{r}},\phi_{\vec{r}})$, whereas $C_m^{(l)}(\theta_{\vec{q}},\phi_{\vec{q}})$ is related to the photon momentum direction ($\hat{q}$) and gives rise to natural (crystal field) dichroism in anisotropic systems.[15] It is to be noted that the sum over l in Eq. (3), enters as a coherent summation into $S(\vec{q},\omega)$ [Eq. (2)], and this results in interferences between the the various l-channels. All this is well exemplified by the observation of d-d transitions in TM compounds by Larson *et al.*,[16] and its subsequent explanation in terms of excitonic transitions by Haverkort *et al.*[13] Even for dipole-allowed transitions like our example of the $5d \rightarrow 5f$ transitions in the actinides, NIXS can access the dipole-forbidden parts of the final state core-valence multiplet and provides a much better representation of the true ground state of the system.[15,17]

As a relevant illustration we show, in the inset to Fig. 1(c), the radial transition probabilities for the various allowed channels in the $5d \rightarrow 5f$ NIXS of the Th^{4+} ($5f^0$) system (relevant for ThO_2), plotted against q, as obtained using Cowan's atomic Hartree-Fock (H-F) code.[18] From the selection rules, this transition has allowed channels for the *dipole* ($l = 1$), *octupole* ($l = 3$) and the *triakontadipole* ($l = 5$) sectors.[19] From Fig. 1(c) we find that the transition probabilities for the three channels peak at very different values of q, and that with increasing q, the cross-section for the dipole transition is suppressed while that for the $l = 3$ first and then for the $l = 5$ sectors are enhanced, at the cost of the dipole. This trend can be understood[13] on the basis of the behavior of $j_l(x)$ as a function of (l,x). With increasing order l, the first largest peak of the spherical Bessel functions occur at progressively larger values of x, and with decreasing absolute intensity. Since the range of r ($x = qr$), that contributes most significantly, is dictated by the range of the associated atomic radial wavefunctions, which is fixed for a given transition, larger values of q are needed to capture peaking at progressively larger x.

The rest of the article is organized as follows. In Sec. II, we summarize the salient features of the experimental NIXS spectra in the early actinide oxides ThO_2 and UO_2. This includes the general q-dependent trends that they exhibit and their comparison with simple renormalized atomic multiplet calculations, as detailed by Bradley *et al.*[20] This already brings out the key issues which we are to address in this article. In Sec. III, we elucidate the reason for the drastic reduction of the Slater-Condon integrals needed, within a simple renormalized atomic multiplet approach, to account for the experimental lineshapes, in terms of final state CI with higher lying levels like the $6f$. Section IV deals with the mechanism for the formation of the GDR, and the reason for the dichotomy between the dipole and higher multipole transitions. It is further

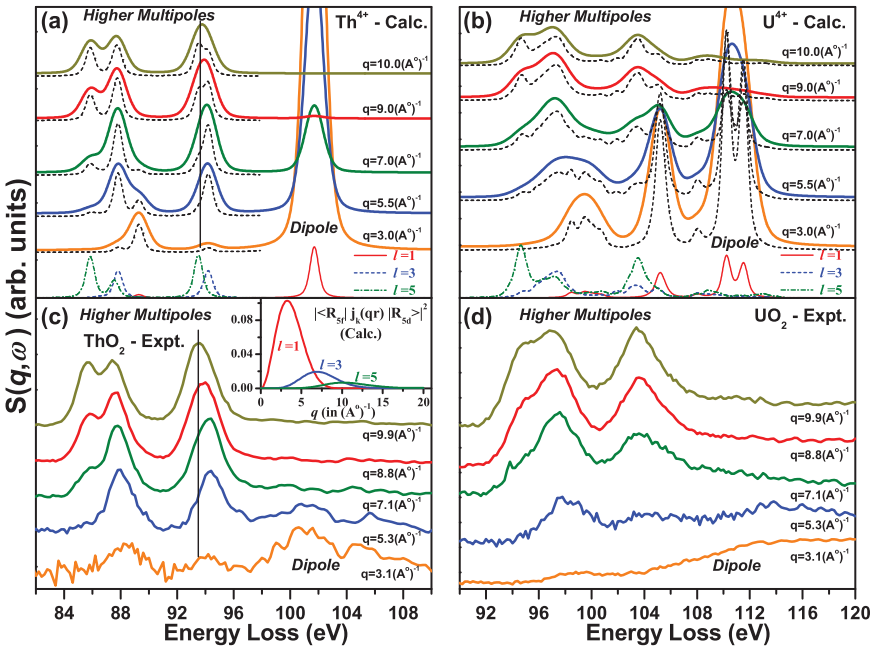

FIG. 1. (Color online) Calculated q-dependent NIXS spectra [$S(\vec{q},\omega)$] within a simple *renormalized atomic multiplet model* for the $5f^0$ system Th^{4+} (a), compared with the corresponding experimental NIXS spectra[20] for ThO_2 (c); and for the $5f^2$ system U^{4+} (b), compared with the corresponding experimental NIXS spectra[20] for UO_2 (d). The respective component spectra (calculated) for the $l = 1,3,5$ channels are shown at the bottom of panels (a) and (b). Also, in each case, the calculated spectra with high resolution (dashed lines) is shown below the calculated spectra with experimental resolution (thick solid lines), to bring out the finer details of the multiplet structure. The inset to panel (c) shows the relative variation of the cross-sections (transition probabilities) for the different multipole channels as a function of q.

subdivided into three subsections: Sec. IV A discusses why transitions within the same principal quantum number shell show markedly different behavior compared to those between different principal quantum number shells, with appropriate examples in each case, also illustrating the generality of the concepts involved; Sec. IV B discusses a model calculation for ThO_2, including both discrete and continuum states, that captures the formation of the GDR; finally, Sec. IV C illustrates how *more-than-half-filled* systems can behave very differently from their *less-than-half-filled* counterparts, and predicts the formation of *giant multipole resonances*. We end the article with the usual *conclusions* and *acknowledgments* sections.

II. $5d$-$5f$ NIXS IN THE ACTINIDES: EXPERIMENT VERSUS RENORMALIZED ATOMIC MULTIPLET THEORY

A detailed description of the experimental trends in the O_{45} edge ($5d-5f$) NIXS of Th ($5d^{10}5f^0 \rightarrow 5d^9 5f^1$) and U ($5d^{10}5f^2 \rightarrow 5d^9 5f^3$), with a brief account of their simulation within a simple renormalized atomic multiplet approach has been provided for various fillings of the $5f$ shell (in the $5f^0$ systems ThO_2 and $Cs_2UO_2Cl_4$, the $5f^2$ system UO_2, and the mixed-valent system U_3O_7) in our earlier article[20] (*c.f.* R. Caciuffo *et al.*).[21] We shall here recount the salient points most relevant to our discussion, for the sake of clarity and completeness. In Fig. 1 are shown the experimental NIXS for ThO_2 (a $5f^0$ system) and UO_2 (a $5f^2$ system) [Fig. 1(c) and 1(d), respectively], compared with the corresponding renormalized atomic multiplet calculations [Fig. 1(a) and 1(b), for Th^{4+} and U^{4+} respectively] plotted with the experimental resolution (solid lines), as a function of q. The calculations were based on an atomic many-body Hamiltonian, $\mathcal{H}_{5d-5f}$, consisting of the onsite energies of the atomic core-$5d$ (ε_{5d}) and valence-$5f$ (ε_{5f}) levels, spin-orbit coupling (ξ_{5f}) and full multiplet Coulomb interactions within the $5f$ manifold [expressed in terms of the non-mixing Slater-Condon integrals (F^0_{ff}, F^2_{ff}, F^4_{ff}, F^6_{ff})], spin-orbit interaction within the core-$5d$ level (ξ_{5d}), and the final state full multiplet core-valence Coulomb interactions [expressed in terms of the non-mixing Slater-Condon integrals (F^0_{df}, F^2_{df}, F^4_{df}, G^1_{df}, G^3_{df}, G^5_{df})]. The spin-orbit and Slater-Condon integrals were computed using Cowan's atomic H-F code and scaled as described below. The qualitative trends are very similar in the two systems and following points summarize the main conclusions :

(i) For low-q, the main feature appears at relatively higher energies and following the trend in the transition probabilities for the various channels, we conclude that it corresponds mainly to dipole transitions. This is also consistent with the fact that for small q, the NIXS operator $e^{i\vec{q}\cdot\vec{r}} \approx 1 + i\vec{q}\cdot\vec{r}$, where the first term does not contribute due to the orthogonality of $|i\rangle$ and $|f\rangle$, while the second term mimics the usual dipole term[22] $\hat{\varepsilon}\cdot\vec{r}$, with $\vec{q}$ playing the role of the polarization $\hat{\varepsilon}$. With increasing q, spectral weight is transferred from the dipole feature to the "pre-absorption edge" higher multipole features at lower energy just as in the inset to Fig. 1(c). The component pure *dipole* ($l = 1$), *octupole* ($l = 3$) and the *triakontadipole* ($l = 5$) features are also shown at the bottom of Figs. 1(a) and 1(b).[19] These, together with the theoretical NIXS spectra plotted with high resolution for each q (dashed lines), show that the *apparent shift* of the broad peak at about 93 eV is actually a spectral weight transfer from the $l = 3$ to the $l = 5$ feature with increasing q. These high resolution spectra also make it amply clear that although the qualitative trends are similar for both the systems, the detailed spectral shape is very different between the two. Thus UO_2 being a $5f^2$ system has additional f-f multiplet interactions in the final state, absent in the $5f^0$ system ThO_2, which yields a more complicated final state multiplet structure for the former, as seen.

(ii) The important point is that the experimental NIXS data for actinides show the dichotomy that the high multipole features are sharp and excitonic, while the Fano-like asymmetric[6] dipole feature is broad, relatively featureless and spread out over a very large energy range.

(iii) In stark contrast, the calculated low-q dipolar NIXS spectra are much sharper and much more intense, just like the lower energy high multipole terms. Thus, the dichotomy mentioned in (ii) above is not captured by the present level of theory.

(iv) Also very importantly, in order to obtain reasonable agreement with experimental peak positions (the dipole peak position is especially extremely sensitive) and relative intensities of the various features within this conventional renormalized atomic multiplet calculation,[20] one needs to drastically scale down the $5d$-$5f$ Coulomb and exchange Slater-Condon integrals (F^k_{df},G^k_{df}), to 60% (ThO_2) and 50% (UO_2) of their atomic H-F values. For UO_2 the $5f$-$5f$ Slater-Condon integrals (F^k_{ff}) were also scaled similarly (*i.e.*, to 50%) but the spectrum was found to be much less sensitive to this compared to the $5d$-$5f$ scaling. This is hard to justify for these rather atomic-like $5f$ wavefunctions.[23,24] Although the $5f$ orbitals are expected to be more covalent than the $4f$, they are definitely more localized than the $3d$ orbitals in the TM compounds for which normally an 80%-85% scaling works very well.[23]

In passing, we note that the dichotomy, discussed in (ii) above, is also observed in the N_{45} ($4d \rightarrow 4f$) NIXS of RE systems[17] and the M_{23} ($3p \rightarrow 3d$) NIXS of TM compounds,[15] and between the *"doubly forbidden"* pre-edge peak and the GDR, in the O_{45} XAS or EELS of actindes,[1,11] showing that this is a generic feature of shallow-core to valence transitions, *i.e.*, within the *same n-shell*. Below we address each of these issues, starting with the issue of the drastic reduction in the Slater-Condon integrals. From now on we shall focus our attention on the $5f^0$ system ThO_2 alone, treating it as a model system where the core-valence multiplet structure in the final state is not unnecessarily complicated by the presence of additional f-f multiplet interactions. This helps bring out the essential physics which is robust and is expected to hold also for other actinide systems, at least the early ones. We shall come back to the case of a late actinide later.

III. POSSIBLE REASON FOR THE DRASTIC REDUCTION OF THE SLATER-CONDON INTEGRALS: CI WITH THE $6f$

To understand the origin of the apparent large reductions in the Slater integrals, we plot in the *top inset* of Fig. 2(a), the $5d$,

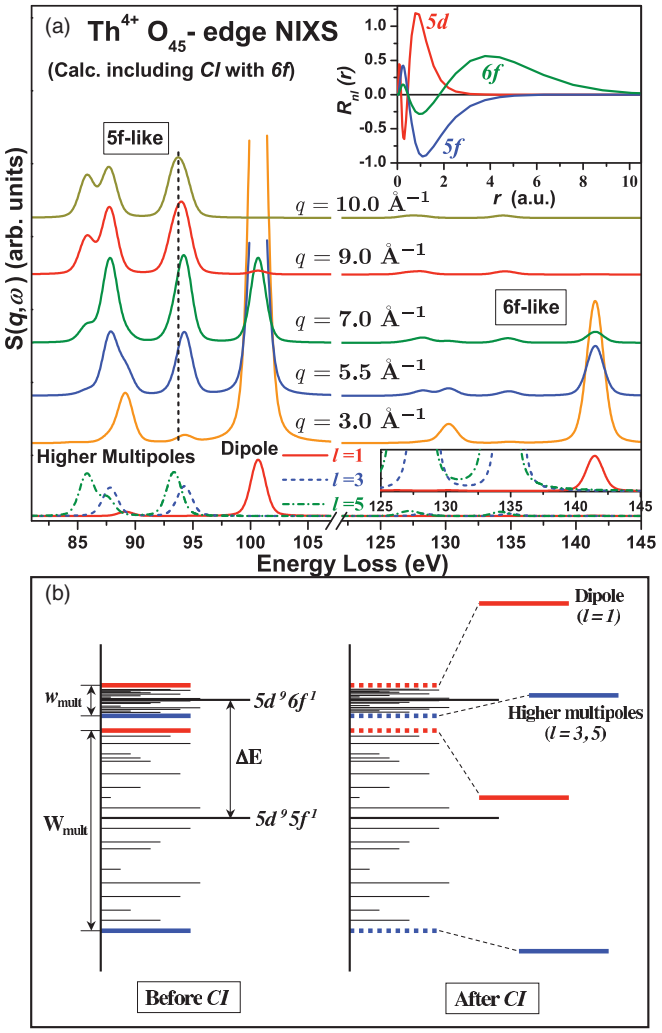

FIG. 2. (Color online) (a) Plots of the $5d$, $5f$, and $6f$ atomic H-F radial wavefunctions for Th^{4+} ($5f^0$ system) (*inset* at the top); and calculated NIXS [$S(\vec{q},\omega)$] for the same, including final-state CI with the $6f$ level, for 60% of atomic $CI(5f\text{-}6f)$ values (*main*). Both the $5f$-like and $6f$-like regions are shown. The bare component (l = 1,3,5) spectra (*not to scale*) are shown at the bottom ($6f$ region magnified in the bottom inset for clarity). (b) Schematic illustrating the high sensitivity of the dipole term vis-a-vis the high multipole terms, due to the strongly term-dependent CI with the $6f$.

$5f$ and the $6f$ radial wavefunctions, obtained from an atomic H-F calculation for ThO_2 (Th^{4+}, ground configuration $5f^0$). The $5d$ and $5f$ orbitals (same n-shell) overlap very strongly, which accounts for the large values of the atomic (F^k_{df},G^k_{df}) integrals. In contrast, the more diffuse $6f$ orbital, with an additional radial node, overlaps only weakly with the $5d$. Hence, if the final state Hilbert space is augmented to include both the $5d^95f^1$ and $5d^96f^1$ configurations, then a CI *via* the $CI(5f\text{-}6f)$ matrix elements,[25] would effectively expand the radial part of the $5f$ wavefunction, which undermines its overlap with the $5d$, in turn reducing the $5d\text{-}5f$ Slater integrals. Now, the mixing depends also on the energy separation, ΔE, between the center-of-gravities of configurations involved, which is smaller in the heavier actinides, than between $4d^94f^1$ and $4d^95f^1$ in the lighter RE ions, for example. This results in a strong multiplet-dependent CI, because the core-valence multiplet splitting of $5d^95f^1$ is much larger than that of $5d^96f^1$, as shown schematically in Fig. 2(b), and which will be discussed in detail below. To illustrate this point, the NIXS spectra for ThO_2 (Th^{4+}) are calculated (using the XTLS8.3 code)[26] on the basis of the aforesaid CI model, for which the Hamiltonian has the structure:

$$\mathcal{H}_{CI} = \begin{pmatrix} \mathcal{H}_{5d-5f} & CI(5f-6f) \\ CI(5f-6f) & \mathcal{H}_{5d-6f} \end{pmatrix}, \qquad (4)$$

where $\mathcal{H}_{5d-6f}$, for the $5d^96f^1$ configuration, has basically the same form as $\mathcal{H}_{5d-5f}$ for the $5d^95f^1$ configuration, discussed earlier, except that the $5f$ level is now replaced by the $6f$ level, and $CI(5f-6f)$ are the configuration interaction Coulomb integrals,[25] which mix the above two configurations. $S(\vec{q},\omega)$ is then calculated as a coherent combination of the NIXS transitions $5f^0 \rightarrow 5d^95f^1$ and $5f^0 \rightarrow 5d^96f^1$. Here we leave the (F^k_{df},G^k_{df}) integrals unaltered at their atomic H-F values, while the scaling of $CI(5f\text{-}6f)$ is varied to obtain agreement with experimental peak positions. This presents a more natural and physical mechanism for understanding the reduced multiplet spread, observed experimentally. The fact that we need to scale the CI integrals merely indicates that the band-like $6f$ state is poorly approximated by the atomic H-F calculations, and that CI with numerous other states is neglected in this minimal model that just serves to bring out the basic physics. The full q-dependent spectra, at the optimized 60% scaling of $CI(5f\text{-}6f)$ [Fig. 2(a)], is spread over a wide energy range and consists of $5f$-*like* and $6f$-*like* regions (marked in the figure), though most of the spectral weight lies in the $5f$-like region due to dominance of radial transition matrix elements. The CI serves to reduce the $5d\text{-}5f$ multiplet spread considerably (while enhancing the $5d\text{-}6f$ spread), especially pushing the dipole peak close to the high multipole peaks, in good agreement with experiments.[20] Also the component spectra for the l = 1,3,5 channels plotted at the base of Fig. 2(a) (vertical scale not to be compared with the actual spectra above) clearly show that it also reproduces the mild shift of the high multipole peak at ~93 eV, due to a q-dependent weight transfer between the $l = 3$ and $l = 5$ channels, as seen in experiments or in the renormalized atomic multiplet calculations[20] (*c.f.* Fig. 1). The dipole states, in general, mix much more and respond much more sensitively to the CI than the high multipole states. This also means that there is a substantial amount of interference between the $5f$-like and $6f$-like dipole transitions. All of this helps to transfer a finite part of the spectral weight from the $5f$-like dipole feature to the $6f$-like one, as seen from Fig. 2(a), but the effect is very small for the high multipole part, which is desirable as it was already in agreement with experiments. However, this is still far from what is needed to convert the very sharp and intense dipole peak in the calculation into the very broad and diffuse GDR seen in the experiments. All of this physics is absent in a simple renormalized atomic multiplet approach,[20] as described above.

The origin of the higher sensitivity of the dipole compared with the higher multipoles is explained schematically in Fig. 2(b). Before CI (left), the difference (ΔE) in the center-of-gravity energies for the two final state multiplet families, $5d^95f^1$ (width $W_{\rm mult}$) and $5d^96f^1$ (width $w_{\rm mult}$),

is ∼23–24 eV, from H-F calculations. Although both the multiplets involve exactly the same terms, $W_{\rm mult}$ (∼25 eV) is much larger than $w_{\rm mult}$(∼7 eV), demonstrating the difference between states involving the *same* versus *different* principle quantum numbers. Also, for a less-than-half-filled system which typically has a low angular momentum (J) ground state, the highest multiplets (*red*) are generally dipole-allowed, while the lowest ones (*blue*) are the high multipole allowed terms. This can be understood with the example of ThO_2, which is a $5f^0$ system in the atomic limit, and has a ^{1}S ($J = 0$) ground state. Thus in the final state configuration $5d^9 5f^1$, which involves Coulomb and exchange interactions between a $5d$ hole and a $5f$ electron, with angular momenta $l_d = 2$, $l_f = 3$ and spin-$\frac{1}{2}$ each, as the dominant effect (neglecting the spin-orbit coupling especially of the core-$5d$, for the time being), one has the possible terms ^{1,3}P, ^{1,3}D, ^{1,3}F, ^{1,3}G, and ^{1,3}H. From the ^{1}S ground state, a dipole transition is possible only to the ^{1}P state, which by virtue of Hund's rules, is one of the highest energy states of the core-valence multiplet structure. On the other hand, the state ^{1}H which is one of the lowest energy terms by virtue of Hund's rules, is reachable from the ground state only by a *triakontadipole* ($l = 5$) transition. Although normally forbidden, most of the triplet states can be reached because of the perturbation by the core-$5d$ spin-orbit coupling.[11] Now $CI(5f\text{-}6f)$ (which consists of the mixing direct and exchange Coulomb integrals $(R^0_d, R^2_d, R^4_d, R^1_e, R^3_e, R^5_e)$, the largest of which is ∼2 eV, even after a reduction to 60% of its atomic value) only mixes terms of the same symmetry,[18] *e.g.*, the red (blue) states at the top (bottom) of $5d^9 5f^1$, mix only with the red (blue) states at the top (bottom) of $5d^9 6f^1$. The result after mixing is shown in the right panel of Fig. 2(b). Since $w_{\rm mult} \ll W_{\rm mult}$, the effective energy denominator for mixing of the red (dipole) terms $[\sim \Delta E - \frac{1}{2}(W_{\rm mult} - w_{\rm mult})]$ is much smaller than that for the blue (high multipole) terms $[\sim \Delta E + \frac{1}{2}(W_{\rm mult} - w_{\rm mult})]$, causing the observed differences in the shifts. Because of these strong correlation effects, the effective "screening" becomes highly term dependent, explaining the strong asymmetry in the behavior of the dipole and the high multipole terms, which is not captured by a uniform reduction of the Slater integrals.[20]

To show that the two approaches are qualitatively different, we compare in Fig. 3(a) the experimental q-averaged NIXS (topmost), with the calculated sum of the three component spectra (l = 1,3 and 5), keeping (F^k_{df}, G^k_{df}) fixed at their atomic values, while the $CI(5f\text{-}6f)$ are switched on and gradually increased to their atomic values (100%) (top to bottom). For this purpose only the peak positions are relevant. As already noted, a good agreement with high multipole peak positions is obtained for 60% scaling of $CI(5f\text{-}6f)$. But more importantly, with a gradual uniform reduction in (F^k_{df}, G^k_{df}) we would expect a linear movement of the dipole toward the high multipole features. On the other hand, with changing degree of CI, the dipole moves toward the high multipole peaks in a nonlinear manner [Fig. 3(a)], showing signs of saturation, as governed by *level-repulsion physics*. This contrasting behavior is shown in Figs. 3(b) and 3(c), where we have plotted the dipole peak position in the two cases, as a function of the scaling of $CI(5f\text{-}6f)$ and of (F^k_{df}, G^k_{df}), respectively.

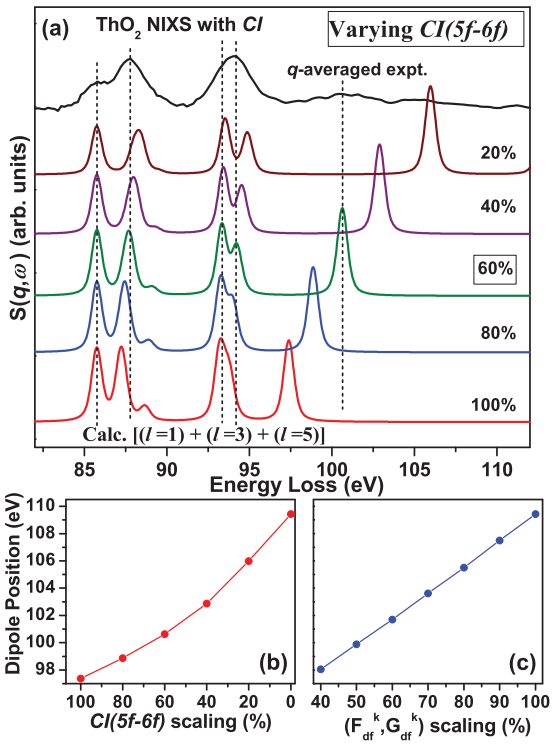

FIG. 3. (Color online) (a) Experimental q-averaged NIXS for ThO_2, compared with the component (l = 1,3,5) summed calculated spectra for atomic values of (F^k_{df}, G^k_{df}), and the $CI(5f\text{-}6f)$ varied from a scaling of 20% to their full atomic values. *Only peak-positions are relevant.* The best agreement is obtained at 60% scaling of $CI(5f\text{-}6f)$. Variation of the high-energy dipole peak position with varying scaling of: (b) $CI(5f\text{-}6f)$, and (c) (F^k_{df}, G^k_{df}). While the latter shows a simple linear trend, the former shows a parabolic behavior with signs of saturation.

IV. ORIGIN OF THE GIANT DIPOLE RESONANCE (GDR) : MIXING WITH CONTINUA AND THE FANO EFFECT

A. Why different transitions behave differently?

We now turn to the problem of the experimentally observed low relative amplitude, large width and non-lorentzian line shape of the GDR. To begin with, we address the question as to why edges involving transitions within the same principal quantum number (n-) shell behave very differently from edges that involve transitions between different n-shells. We note that although for the former case, the dominant interaction in the final state is the multiplet core-valence Coulomb interaction which is larger than the core-hole spin-orbit coupling, for the latter the core-hole spin-orbit coupling is the largest energy, followed by the core-valence Coulomb interaction.

To this end we perform a simple gedanken experiment, as illustrated in Figs. 4(a)–4(d). For both XAS and NIXS, if the initial valence state was nl^m (*e.g.*, $5f^m$), with m electrons in the valence shell (principal quantum number n, and sub-shell l), then the final state valence configuration is nl^{m+1} (*e.g.*, $5f^{m+1}$), in the presence of a core-hole $n'(l-1)$ (*e.g.*, $\underline{5d} \equiv 5d^9$ or $\underline{4d} \equiv 4d^9$), the underline denoting a hole state. Although NIXS can access dipole forbidden edges also in general, we have here restricted ourselves to dipole-allowed edges in taking $l' = l - 1$, as we want to bring out the dichotomy between the

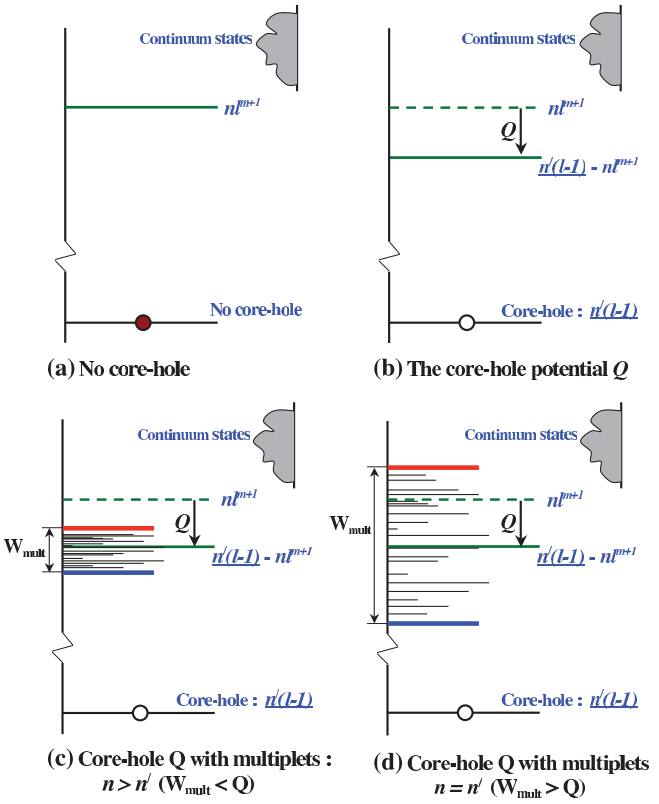

FIG. 4. (Color online) Schematics illustrating the differences between transitions occurring between different n-shells and within the same n-shell (see text): (a) The final valence state of XAS or NIXS in the absence of the core-hole; (b) the effect of a scaler core-hole potential (Q) on this final state; (c) its fanning out due to core-valence multiplet effects, in the case $n > n'$, when all final state terms are excitonic bound states; and (d) formation of the core-valence multiplet in the case when $n = n'$, leading to a gradual crossover from bound-states (lower terms) to virtual-bound resonances (higher terms) as a function of energy.

dipole-allowed and high multipole terms under the special circumstance when $n' = n$. The aforesaid state is shown in Fig. 4(a), but in the absence of the core-hole (formally identical with the final state of inverse photoemission on a nl^m state), when it is positioned below or just inside a continuum (the continuum could relate to band-structure or autoionization continua *etc.*). Now, suppose the core-hole is created at this site [Fig. 4(b)]. To start with, we assume that its only effect is to provide an attractive scalar potential, that pulls down the nl^{m+1} level by an amount Q, on the average, and this is now referred to as the [$n'(l-1)$-nl^{m+1}] (*e.g.*, $\underline{5d}$-$5f^{m+1}$) state. The potential Q is often strong enough to pull down this level below the continuum. However, this is not the sole effect of the core-hole and the multipole part of the core-valence Coulomb interaction gives rise to a fanning out of this state into a multiplet structure of width $W_{\rm mult}$. The level [$n'(l-1)$-nl^{m+1}] is now understood to be the center-of-gravity of this newly formed multiplet structure. Now, two disparate situations can arise as is illustrated in Figs. 4(c) and 4(d), *viz.*: (i) where transitions occur between subshells belonging to two different principal shells (Fig. 4(c) where $n > n'$, *e.g.*, $4d^9 5f^{m+1}$). Here, the Slater-Condon integrals that decide $W_{\rm mult}$ are relatively small as the core and the valence levels belong to different n-shells, and hence $W_{\rm mult} < Q$. Then, as shown in Fig. 4(c), all the final-state multiplets (both dipole and high multipole) are situated well below the continuum and form bound *core-hole excitonic states*, that can be treated within local models. Such is the case for the celebrated $2p \rightarrow 3d$ transitions in the TM oxides or $3d \rightarrow 4f$ transitions in the RE compounds, where XAS works so very well. (ii) More interesting is the case where they belong to the same n-shell [Fig. 4(d), where $n = n'$, *e.g.*, $5d^9 5f^{m+1}$]. In this case, the Slater-Condon integrals are very large due to the large overlap between these orbitals, and $W_{\rm mult} > Q$. Then, as in Fig. 4(d), the high multipole terms toward the bottom of the multiplet, still form excitonic bound states, but the dipole-allowed terms in the highest part of the spectrum are pushed up by a large amount, offsetting the attractive effect of Q, and now lie well within the continuum. Once they are degenerate with some of the continuum states, they can easily mix with them, and this gives rise to very broad and asymmetric *excitonic resonances* with characteristic Fano lineshapes.[27] This physical picture clearly demonstrates why the dipole and the high multipole states show a crossover from virtual-bound to bound excitonic character, at edges involving transitions within the same n-shell. This is the case for the $5d \rightarrow 5f$ edges in the actinides,[20] the $4d \rightarrow 4f$ edges in the RE compounds,[17] or the $3p \rightarrow 3d$ edges in TM compounds.[15]

B. A model calculation illustrating the formation of the GDR

With this understanding of the origin of the dichotomy between the dipole and the high multipole features, we shall now try to understand, in some more detail, the lineshape of the GDR. As we have already pointed out, the GDR has a typical Fano-like asymmetric lineshape.[6] A Fano line-shape arises when there coexists a discrete state which is degenerate with a continuum and one considers transitions to both of these states from a third (discrete) state. Due to the mixing of the former discrete state with the continuum, these two transitions can interfere giving rise to a very broad and asymmetric lineshape.[6]

Thus, to simulate the $5d$-$5f$ NIXS of ThO_2, we consider the model shown in Fig. 5(a), which is an extension of our earlier model for the CI. As shown, it consists of the core $5d$, the valence $5f$ and the empty $6f$ levels on Th. The interaction of the $5f$ with the $6f$ and the transitions to the $6f$ are not shown in the figure, although included in the calculation, as it has been discussed before and does not shed any extra light on the physics we are about to discuss. Instead we just show the fanning out of the renormalized $5d^9 5f^1$ multiplet structure after the CI with $5d^9 6f^1$ has been taken into account. However, now in addition we also include in the calculation, a fictitious discretized $7p$-like band spreading over an energy range of 7 eV. The discretization step used was 0.2 eV, so that the degeneracy was $N_p = 36$. The band is positioned to start below the high energy dipole term, but above the high multipole terms, as shown. We consider NIXS transitions from the $5d$ core-level to the $5f$-level (denoted by T_{5d-5f} and has allowed transitions in the $l = 1,3,5$ channels) as well as to the states in the $7p$-like continuum (denoted by T_{5d-7p} and has allowed transitions in the $l = 1,3$ channels). The terms in the

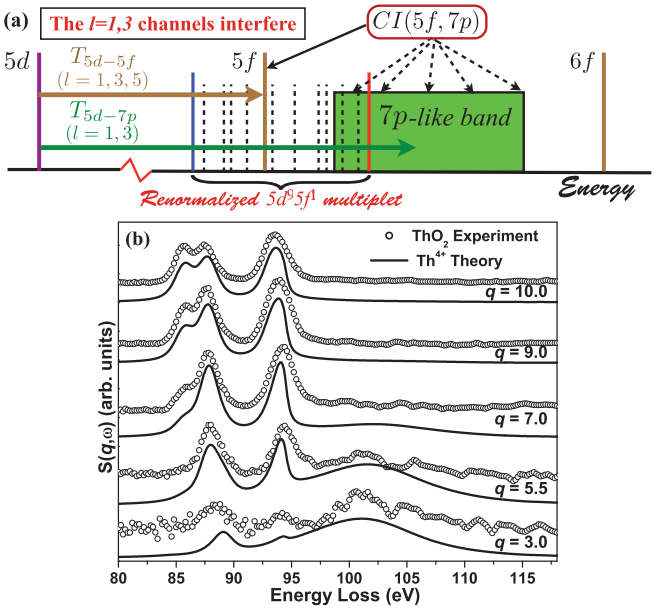

FIG. 5. (Color online) (a) Schematic showing the model used to simulate the O_{45} NIXS of ThO_2 (Th^{4+}), which captures both the excitonic high multipole features as well as the GDR. It includes a Fano-effect of the mixing of the atomic $5d$-$5f$ transition, with that to a fictitious $7p$-like rectangular broad band, via the $CI(5f\text{-}7p)$ matrix elements. (b) The calculated $S(\vec{q},\omega)$ from the model (lines) resulting in a broad, asymmetric lineshape for the high-energy dipole term, that agrees well with the experimental q-dependent NIXS for ThO_2 (symbols).[20] A dipole term at lower energy (~89 eV) is not broadened into a resonance, but appears as an excitonic feature just like the high multipole terms.

$5d^95f^1$ multiplet mix (hybridize) with the continuum states via the $CI(5f\text{-}7p)$ Coulomb matrix elements[25] which are similar to the $CI(5f\text{-}6f)$ matrix elements introduced earlier. Both the transition matrix elements, T_{5d-7p}, as well as the mixing matrix elements $CI(5f\text{-}7p)$ were scaled using the usual $1/\sqrt{N_p}$ factor. An additional overall scaling factor was used to optimize the mixing matrix elements $CI(5f\text{-}7p)$ to obtain good agreement with experiments. From the definition of the Fano-effect in the last paragraph, it is apparent that the $l = 1,3$ channels, present in both the transitions, can interfere via the $CI(5f\text{-}7p)$ matrix elements, and give rise to a Fano-effect.[6]

In Fig. 5(b) we show the calculated $S(\vec{q},\omega)$ for Th^{4+}, from this model (lines). We find that while the lower lying $l = 3,5$ peaks remain sharp and excitonic, the high-energy dipole feature forms a GDR, just as discussed in the last section. Interestingly, a dipole-allowed peak present at lower energy (~89 eV) is not broadened by this mechanism, implying that *the position within the multiplet, rather than the symmetry of the state, decides its fate*. In the same figure we have also shown the experimental q-dependent NIXS spectra (symbols). A fairly good comparison with the experimental spectra[20] is obtained if we use a somewhat larger Lorentzian width for the GDR compared to the high multipole states, to simulate the multiplet dependent core-hole decay probabilities, not included in the present calculation.

C. A *more-than-half-filled* system can behave differently: Example of giant multipole resonances in Tm^{3+}

In the last section we showed that the position within the multiplet, rather than the symmetry of the state, decides its fate. Here we elucidate this further with the example of a more-than-half-filled model rare-earth system Tm^{3+}, which is relevant for the oxide Tm_2O_3. The ionic configuration in the ground state is $4f^{12}$ and the N_{45} NIXS involves the transition $4d^{10}4f^{12} \rightarrow 4d^94f^{13}$. This makes the final state particularly simple (a two-hole state), hence the choice. The $4f^{12}$ system has a high J ground state given by the term $^3H_6$ ($J = 6$). However, the final state configuration $4d^94f^{13}$ has the same terms as the final state for the $5f^0$ system, *viz.* ^{1,3}P, ^{1,3}D, ^{1,3}F, ^{1,3}G, and ^{1,3}H ($L = 1,2,3,4,5$; $S = 0,1$). Starting from the $J = 6$ ground state, dipole transitions can occur only to final states with $J = 5$ (no $J = 7$ state is possible here), which could either be a state like $^3G_5$ ($L = 4, S = 1$) or to the states $^{1,3}H_5$ ($L = 5, S = 0,1$). These terms with relatively high L and S values, are expected to be some of the low lying states of the multiplet, by Hund's rules. On the other hand, some of the highest terms are expected to be the ones like ^{1,3}P or ^{1,3}D *etc.*, which can be reached only by triakontadipole ($l = 5$) or octupole ($l = 3$) transitions. This is indeed borne out by actual calculations as shown in Fig. 6(a), where we show calculated component spectra for the three ($l = 1,3,5$) channels from a renormalized atomic multiplet calculation (f-f and d-f Slater-Condon integrals reduced to 80% of atomic values). We find that in the multiplet

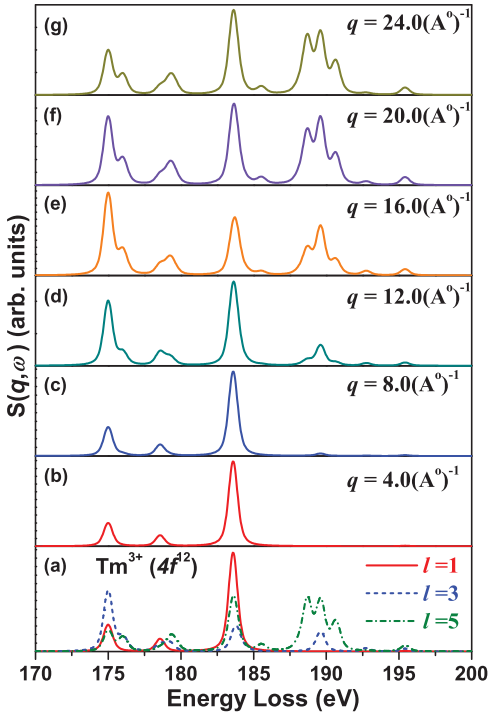

FIG. 6. (Color online) Calculated N_{45} NIXS for a model more-than-half-filled rare-earth system Tm^{3+}, (*e.g.*, in Tm_2O_3). The transition involved is $4d^{10}4f^{12} \rightarrow 4d^94f^{13}$. (a) The bare component spectra for the $l = 1,3,5$ channels. (b)-(g) Calculated NIXS spectra [$S(\vec{q},\omega)$] plotted as a function of increasing q, for $q = 4,8,12,16,20$, and 24 $Å^{-1}$. The vertical scales in the different panels are not to be compared.

structure which is spread out over 25 eV or more, the dipole channel indeed reaches some of the lowest states between 175-179 eV and even the highest dipole term lies at about 184 eV, which is still much lower in energy than the octupole and triakontadipole allowed terms lying between 188-196 eV.

In Figs. 6(b)–6(g), we show the full NIXS spectra $[S(\vec{q},\omega)]$ plotted as a function of q. Note that compared to the $5f$, actinide systems, we need much higher q values to reach the predominantly $l = 3$ or $l = 5$ transitions. This has to do with the fact that the $4f$ has a much smaller radial extent (r) compared to the $5f$, and hence much higher q values are needed to reach the peaks of $j_3(qr)$ and $j_5(qr)$. From Fig. 6, it is clear that the aforesaid dichotomy between the dipole and the high multipoles (as seen in the early actinides), may be reversed in cases where the dipole allowed states are lower in energy than the high multipoles, like for more-than-half-filled systems, which have large ground state J values. In such cases one can expect sharp, excitonic peaks for the dipole terms, while some of the high multipole allowed terms at higher energies may be broadened into resonances, due to mixing with continuum states. This opens up the possibility of observing *giant octupole or triakontadipole resonances* instead of the more common GDR.

V. CONCLUSIONS

In conclusion, we have shown that the modeling of same *n-shell* NIXS is complicated by the simultaneous presence of virtual-bound and bound states within the same final-state multiplet. The complex virtual-bound resonances, involving non-local effects, provide insight into the hybridization of the locally excited core-electron with continua, and about core-hole decay processes. The dipole-forbidden bound states (not prominent in XAS) are modeled using a local, atomic CI approach, that provides direct ground state information. We also explain the apparent strong reduction of the atomic Slater integrals in the final state, which effectively become term dependent, by invoking CI with higher lying empty levels. For *less-than-half-filled* systems with low J ground states, the dipole allowed terms form virtual-bound resonances giving rise to the GDR, while the high multipole terms form excitonic bound states. In contrast, we show with an example, that for *more-than-half-filled* systems with high J ground states, it is possible that this trend is reversed to yield excitonic dipole terms and *giant multipole resonances*. It would be interesting to observe this experimentally.

The excitonic high multipole transitions and especially their angular dependence in single crystal studies[13,15,16] are also expected to provide detailed information on the importance of "orbital-ordering" in the ground state, and changes at phase transitions in "hidden order" materials like URu_2Si_2 [Ref. 3]. The term "hidden order" refers normally to ordering of high angular momentum, many-body wave-functions in the compounds of heavier elements, which could be of "pure orbital" or of "mixed spin-orbital" origin. Such ordering is usually invisible to techniques like XAS, involving pure dipole transitions. For example, a dipole transition measured on a material with local cubic symmetry shows no linear dichroism. This is related to the fact that a transition of angular momentum $l = 1$ in spherical symmetry, has only one irreducible representation in cubic symmetry, namely t_{1u}. With a dipole transition, one thus cannot see a difference between the cubic [111] and [001] directions. An f ground-state wave-function, however, might be very different in these two directions. The f states branch down to states of a_{2u}, t_{1u} and t_{2u} symmetry, which are inherently very anisotropic. Similarly, an octupole transition ($l = 3$) branches down to transitions of a_{2u}, t_{1u} and t_{2u} symmetry. Thus, there are three different fundamental spectra and there might very well be a difference between the inelastic scattering with q in the [111] and [001] directions. With the use of higher multipole transitions in NIXS, it is thus possible to observe higher multipole ordering, not observable with a dipole transition. Such studies are under progress.

Finally, the virtual-bound resonances are modeled with an additional term, mixing the $5f$ states with a model conduction band continuum, resulting in their broad and Fano-like line shapes. More realistic approaches to the latter would involve an energy-dependent hybridization with a realistic density of states, and the inclusion of explicit core-hole decay processes. This is a topic of future investigations.

ACKNOWLEDGMENTS

SSG and GAS acknowledge funding from the Canadian agencies NSERC, CFI and CIFAR. GTS and JAB acknowledge support from University of Washington, and the US Department of Energy.

*subhra@phas.ubc.ca

[1] K. T. Moore and G. van der Laan, Rev. Mod. Phys. **81**, 235 (2009).

[2] S. S. Hecker, in *Challenges in Plutonium Science*, Vol. II, (Los Alamos Science, Los Alamos, 2000).

[3] T. T. M. Palstra, A. A. Menovsky, J. van den Berg, A. J. Dirkmaat, P. H. Kes, G. J. Nieuwenhuys, and J. A. Mydosh, Phys. Rev. Lett. **55**, 2727 (1985); V. Tripathi, P. Chandra, and P. Coleman, Nature Phys. **3**, 78 (2007); K. Haule and G. Kotliar, *ibid.* **5**, 796 (2009).

[4] D. van der Marel and G. A. Sawatzky, Phys. Rev. B **37**, 10674 (1988).

[5] *Core Level Spectroscopy of Solids*, by F. de Groot and A. Kotani (CRC Press, Taylor & Francis Group, Boca Raton, London & New York, 2008).

[6] U. Fano, Phys. Rev. **124**, 1866 (1961).

[7] H. Ogasawara and A. Kotani, J. Phys. Soc. Jpn. **64**, 1394 (1995).

[8] It is important to note that such a mechanism, relying on the coupling of the $5d$ photo-excited state to the $5f$ PES continuum *via* super-Coster-Kronig channels, is not operative for a $5f^0$ system[9] like ThO_2, as discussed here.

[9] M. Richter, M. Meyer, M. Pahler, T. Prescher, E. V. Raven, B. Sonntag, and H. E. Wetzel, Phys. Rev. A **39**, 5666 (1989).

[10] G. Wendin, in *Giant Resonances in Atoms, Molecules and Solids*, Vol. 151 of NATO Advanced Study Institute, Series B: Physics (Plenum, New York, 1987).

[11]K. T. Moore and G. van der Laan, Ultramicroscopy **107**, 1201 (2007).

[12]See for example, *Advanced Quantum Mechanics* by J. J. Sakurai (Addison Wesley, Boston, Massachusetts, 1967); and *Electron Dynamics by Inelastic X-Ray Scattering* by W. Schuelke (Oxford University Press, New York, 2007).

[13]M. W. Haverkort, A. Tanaka, L. H. Tjeng, and G. A. Sawatzky, Phys. Rev. Lett. **99**, 257401 (2007).

[14]Michel van Veenendaal and M. W. Haverkort, Phys. Rev. B **77**, 224107 (2008).

[15]R. A. Gordon, M. W. Haverkort, Subhra Sen Gupta, and G. A. Sawatzky, J. Phys.: Conf. Ser. **190**, 012047 (2009).

[16]B. C. Larson, Wei Ku, J. Z. Tischler, Chi-Cheng Lee, O. D. Restrepo, A. G. Eguiluz, P. Zschack, and K. D. Finkelstein, Phys. Rev. Lett. **99**, 026401 (2007).

[17]R. A. Gordon, G. T. Seidler, T. T. Fister, M. W. Haverkort, G. A. Sawatzky, A. Tanaka, and T. K. Sham, Europhys. Lett. **81**, 26004 (2008).

[18]*The Theory of Atomic Structure and Spectra* by R. D. Cowan (University of California Press, Berkeley and Los Angeles, California, 1981).

[19]We would like to stress that the pole of the transition and the change of angular momentum of the one particle wave functions are not one-to-one equivalent. In the examples shown in Fig. 1, the initial orbital is a $5d$ orbital and thus $l_i = 2$. The final state orbital is a $5f$ orbital, so that $l_f = 3$. We find that $\Delta l = l_f - l_i = 1$, is possible not only for the *dipole* transition, but also for the *octupole* and *triakontadipole* transitions. The relation that has to be fulfilled is that the *vectorial sum* of the angular momentum of the *initial orbital*, *final orbital* and *pole* of the transition has to be *zero*. In our case one has to be able to make a closed triangle (triangle relations) of a vector of length 2 [for the initial state orbital with $l_i = 2$ (d orbital)], a vector of length 3 [for the final state orbital with $l_f = 3$ (f orbital)], and a vector of the length of the *pole* of the transition. This can be done for $|l_f - l_i| \leqslant l \leqslant (l_f + l_i)$, which together with conservation of parity leads to the selection rules that a d to f transition can be made with only a *dipole*, *octupole* or *triakontadipole* transition.

[20]J. A. Bradley, S. Sen Gupta, G. T. Seidler, K. T. Moore, M. W. Haverkort, G. A. Sawatzky, S. D. Conradson, D. L. Clark, S. A. Kozimor, and K. S. Boland, Phys. Rev. B **81**, 193104 (2010).

[21]R. Caciuffo, G. van der Laan, L. Simonelli, T. Vitova, C. Mazzoli, M. A. Denecke, and G. H. Lander, Phys. Rev. B **81**, 195104 (2010).

[22]Note that this Taylor expansion of $e^{i\vec{q}\cdot\vec{r}}$ is *not* equivalent to the multipole expansion enumerated in Eq. (3) on a term by term basis. This is easily seen from the fact that, *e.g.*, the 1st term of the Taylor expansion yields the matrix element $\langle f|1|i\rangle$ which is zero except for the case $|i\rangle = |f\rangle$, whereas the first term of the multipole expansion involves the matrix element $\langle f|j_0(qr)|i\rangle$, where $j_0(x) = sinx/x$ is not a constant but a function of x, and this allows transitions between the states nl and $n'l$ (with the additional selection rules $\Delta l = 0$, $\Delta m = 0$). It also turns out that the *constant* and the *quadratic* terms of the Taylor expansion are linear combinations of the *monopole* and *quadrupole* terms from the multipole expansion, *etc.* For small q, the dipole term of the multipole expansion however coincides with the linear term of the Taylor expansion.

[23]E. Antonides, E. C. Janse, and G. A. Sawatzky, Phys. Rev. B **15**, 1669 (1977); **15**, 4596 (1977).

[24]B. T. Thole, G. van der Laan, J. C. Fuggle, G. A. Sawatzky, R. C. Karnatak, and J.-M. Esteva, Phys. Rev. B **32**, 5107 (1985); H. Ogasawara, A. Kotani, and B. T. Thole, *ibid.* **44**, 2169 (1991).

[25]In our case, the $CI(\alpha\text{-}\beta)$ matrix elements refer to the Slater-Condon Coulomb mixing integrals $R^k(5d,\alpha,5d,\beta)$.

[26]A. Tanaka and T. Jo, J. Phys. Soc. Jpn. **63**, 2788 (1994).

[27]The mixing with continua is the most important effect, while the Fano effect is secondary. We find that lineshapes do not change much when transitions to the continuum are switched off.